Available online at www.sciencedirect.com
SCIENCE DIRECT®
Chemical Physics Letters 374 (2003) 222–228
CHEMICAL PHYSICS LETTERS
www.elsevier.com/locate/cplett

Growth behavior of carbon nanotubes on multilayered metal catalyst film in chemical vapor deposition

H. Cui [a,*], G. Eres [a], J.Y. Howe [b], A. Puretkzy [a], M. Varela [a], D.B. Geohegan [a], D.H. Lowndes [a]

[a] *Condensed Matter Sciences Division, Oak Ridge National Laboratory, Bethel Valley Road, Bldg. 3150, Oak Ridge, TN 37831-6065, USA*
[b] *Metals and Ceramics Division, Oak Ridge National Laboratory, Bethel Valley Road, Bldg. 4508, Oak Ridge, TN 37831-6065, USA*

Received 31 July 2002; in final form 16 December 2002

Abstract

The temperature and time dependences of carbon nanotube (CNT) growth by chemical vapor deposition are studied using a multilayered Al/Fe/Mo catalyst on silicon substrates. Within the 600–1100 °C temperature range of these studies, narrower temperature ranges were determined for the growth of distinct types of aligned multi-walled CNTs and single-walled CNTs by using high-resolution transmission electron microscopy and Raman spectroscopy. At 900 °C, in contrast to earlier work, double-walled CNTs are found more abundant than single-walled CNTs. Defects also are found to accumulate faster than the ordered graphitic structure if the growth of CNTs is extended to long durations.

1. Introduction

Carbon nanotubes (CNTs) have unique electronic, mechanical, and thermal properties – including ballistic conduction and the highest known tensile strength and thermal conductivity – which are expected to find applications in electronics and composite materials. However, in order to realize their potential, it is important to understand the nucleation and growth processes of CNTs and, for some applications, to find ways to directly control their synthesis in useful configurations. For example, although the pulsed-laser vaporization method can produce a high yield of single-walled carbon nanotube (SWCNT) bundles [1], laborious purification and separation are required before they can be used or their properties studied, and the SWCNT ends are notoriously difficult to locate for direct studies of nucleation and growth.

In contrast, catalytically controlled chemical vapor deposition (CVD) is promising for nucleation and growth studies, but also is quite versatile for scaled-up production of CNTs. For example, it has been demonstrated that a variety of

* Corresponding author. Fax: +1-865-576-3676.
E-mail address: cui@ornl.gov (H. Cui).

0009-2614/03/$ - see front matter © 2003 Elsevier Science B.V. All rights reserved.
doi:10.1016/S0009-2614(03)00701-2

hydrocarbon species can be used as the carbon source for CVD growth of CNTs, including CH_4 [2–9], C_2H_4 [10,11], C_2H_2 [11–14], C_6H_6 [15], xylene [16,17], thiophene [15], *n*-hexane[18] and CO [10,13,19–21]. A lower partial pressure of carbon supply gas also was demonstrated to be a limiting step for SWCNT growth, and to favor the production of cleaner CNTs with fewer defects [14]. Transition metals including Fe, Co and Ni act as the catalyst for CNT growth in quite different precursor forms such as an evaporated film on a flat substrate [22], an oxide in porous materials [3,4], or suspended in the gas phase [18]. Additives such as Mo and Ru can be used to dilute the catalyst and are found to increase the production and improve the quality of CNTs [3–8,19,21,23].

Of primary interest for the work reported here, the catalytically controlled CVD growth of CNTs on a flat substrate can easily differentiate both ends of the nanotubes, thus facilitating nucleation and growth studies. A multilayered metal-film catalyst of aluminum/iron/molybdenum recently has been reported to control the density of SWCNTs and aligned multi-walled CNTs grown on silicon substrates [7]. However, the temperature-dependence and the time-dependence of growth – two of the most important parameters for controlled synthesis of CNTs – were not reported in that work. In this letter, we have utilized this multilayer catalyst as an easily formed model catalyst that permits controlling the concentration of the active catalytic element (Fe). We report results of a comprehensive investigation of the effects of growth temperature and time on the CVD nucleation, growth and structural type of CNTs while using acetylene (C_2H_2) as the carbon supply gas.

2. Experimental

Electron beam evaporation was employed to deposit the multilayered catalyst structures on 1 cm^2 silicon substrates. Aluminum with a thickness of 10 nm was evaporated first, followed by 1 nm iron, and finally 0.2 nm molybdenum. A piece of the silicon substrate was then placed in an alumina boat, and subsequently transferred into a CVD reactor, which consists of a one-stage furnace and a 1.5 in. O.D. quartz tube. A mixed gas flow of argon (500 sccm) and hydrogen (100 sccm) was used to purge the tube while the furnace was heated up to the desired temperature. In about one hour or when the furnace temperature had stabilized, 2 sccm acetylene was introduced into the gas flow to start the deposition. After the growth process, the acetylene gas flow and the furnace were switched off at the same time. Argon and hydrogen continued to flow until the substrate temperature cooled below 300 °C. The substrate was then taken out of the reactor for analysis. The substrate was broken into halves near the center, so that both the surface and cross-section of the carbon deposit could be examined using high-resolution field emission scanning electron microscopy (FESEM, Hitachi S4700). Carbon deposits also were extensively characterized using Raman spectroscopy (633 nm excitation wavelength) and transmission electron microscopy (TEM, Philips EM400, 100 keV; Hitachi HF2000, 200 keV). The surface morphology of the catalyst on the substrate was observed using atomic force microscopy (AFM).

3. Results and discussion

CNT growth was investigated at different temperatures ranging from 500 to 1100 °C. Fig. 1 shows the cross-section FESEM images of CNTs after 20 min growth. CNTs were not observed on the substrate at 500 °C. Multi-walled carbon nanotubes (MWCNTs) were observed at 600 °C, as shown in Fig. 1a. Although the majority of MWCNTs were vertically aligned (simply due to crowding) with a length of about 1 μm, some MWCNTs appeared to be longer than 3 μm. At 700 °C, aligned MWCNTs dramatically reached a length of about 54 μm (Fig. 1b). With a further temperature increase to 800 °C, however, the length of CNTs decreased, without vertical alignment because of their decreased density and absence of crowding, and some CNT bundles started to appear (Fig. 1c) with their length estimated to be about 10 μm. More CNT bundles can be observed at 900 °C (Fig. 1d), suggesting that multi-walled CNTs with quite small diameters or even

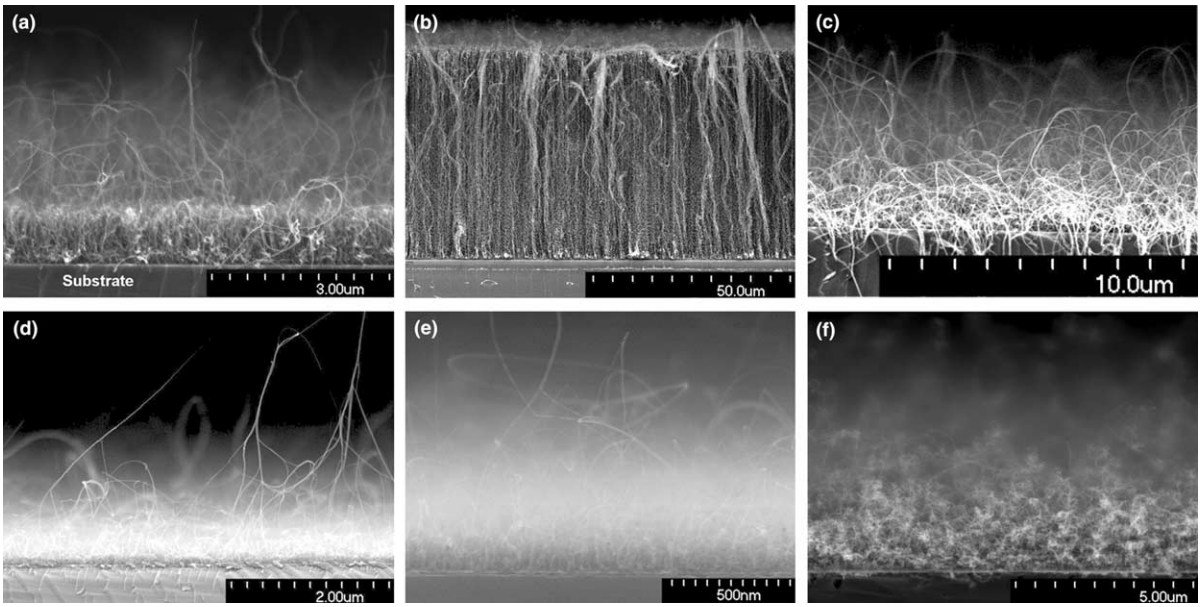

Fig. 1. Cross-section FESEM images of CNTs at different growth temperatures: (a) 600 °C; (b) 700 °C; (c) 800 °C; (d) 900 °C; (e) 1000 °C; and (f) 1100 °C. (d) and (e) are less clear because of the lower density and curved nature of the CNTs, resulting in fewer CNTs in the SEM's focal plane (see Fig. 2 for confirmation).

SWCNTs exist (see the HRTEM and Raman discussion below for their identification). It should be noted that these bundles are formed from CNTs emerging from different growth sites. Furthermore, some CNTs can separate from a bundle after it is formed and incorporate into another bundle nearby, producing CNT networks [2,4]. Bundles with large diameters can be observed to extend upward from the surface, and others appear to form close to the substrate with random direction. The visual appearance of the deposit at 1000 °C appears lighter and much more diffuse than at 900 °C, revealing less surface coverage and consequently still less crowding and vertical alignment. Both the CNT length and nucleation density were reduced at 1000 °C as revealed by Fig. 1e. When the temperature was increased to 1100 °C, however, the substrate surface was found to be densely occupied by curly carbon structures, showing that the carbon deposit is highly defective (Fig. 1f) [14].

Typical CNT morphologies were further observed as a function of temperature and at high resolution by using TEM as shown in Fig. 2. Fig. 2a shows that at 600 °C, CNTs are multi-walled and highly defective. At 700 °C, CNTs also are observed but with smaller diameters and fewer graphitic layers, as shown in Fig. 2b. Double-walled CNTs (DWCNTs) have an amorphous graphitic layer on their outer wall, but their existence is sparse. At 800 °C, SWCNTs begin to appear but are mixed with DWCNTs as well as MWCNTs with more than two graphitic layers (Fig. 2c). A similar mixture is also found at 900 °C. However, DWCNTs appear to be much more abundant than SWCNTs (Fig. 2d), so that the concentration of SWCNTs is small in contrast to results reported by others using this catalyst [7]. The diameter of the SWCNT in the figure is near 1.2 nm, and the DWCNTs near 2.2 nm. It is noteworthy to point out that the MWCNTs have large inner shell diameters and just a few graphitic layers. When the temperature is further increased to 1000 °C (Fig. 2e), carbon fibers with larger diameters are found among smaller nanotubes. Compared with CNTs, the fibers have no distinct wall structure and hollow cavities, thus showing their highly defective (tending toward amorphous) nature. Carbon fibers appear to be the only product at 1100 °C (Fig. 2f).

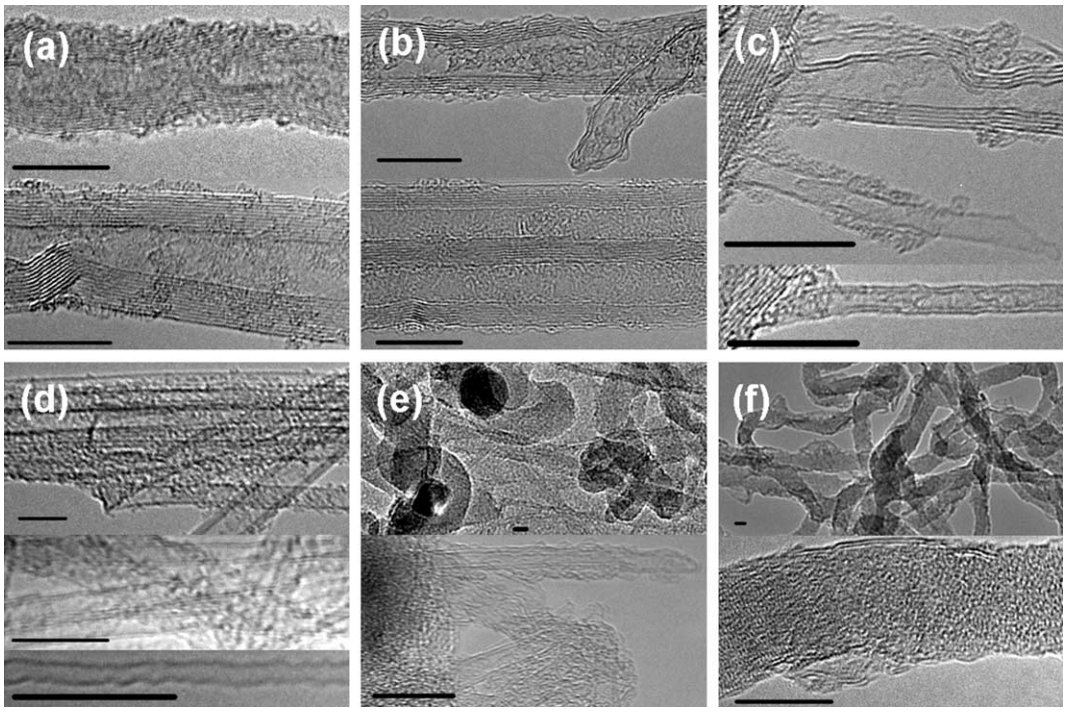

Fig. 2. TEM images of CNTs deposited at different growth temperatures: (a) 600 °C; (b) 700 °C; (c) 800 °C; (d) 900 °C; (e) 1000 °C; and (f) 1100 °C. The scale bar is 10 nm.

Raman spectroscopy was performed on the surfaces of the carbon deposits to characterize the diameter distributions of the smaller CNTs and their graphitic ordering, and to provide statistical information to supplement both the FESEM and HRTEM observations. Each spectrum is comprised of 100 acquisitions with each acquisition lasting 1 second. The CNT growth duration was 20 min at each temperature. As shown in Fig. 3, breathing mode signals in the 100–300 cm^{-1} range were observed between 800 and 1000 °C, reaching a maximum at 900 °C (see insert a and b). The breathing mode signals disappear both at low temperatures (at and below 700 °C) and at higher temperatures (above 1000 °C). The inset a of Fig. 3 shows a detailed breathing mode Raman spectrum at 900 °C with the positions of major peaks marked. At a first-order approximation, if the relationship between the SWCNT diameter D and Raman shift ω, D (nm) $= 248/\omega$ (cm^{-1}) [24], is applied, then the numerical majority of SWCNTs are found to have a diameter distribution between 1.1 and 2.2 nm. Both CNTs with smaller diameter than 1.1 nm and larger than 2.2 nm may also exist at low concentration, according to the Raman spectra. However, this result must be modified when DWCNTs are considered since they appear much more abundant than SWCNTs in HRTEM. Indeed, the DWCNTs can contribute to the breathing mode spectra and cause the peaks to shift [25]. However, the relationship between DWCNT diameter and Raman frequency shift is unknown at this time. The inset b of Fig. 2 shows the relationship of the peak intensity ratio of the G band and the D band as a function of growth temperature, revealing the degree of graphitic ordering in the carbon deposits. Corresponding to the largest breathing mode signal, the carbon deposit at 900 °C also shows a strong G band at 1590 cm^{-1} and weak D band at 1317 cm^{-1} with I_G/I_D reaching a maximum, firmly establishing that CNTs with highly ordered graphitic structures are produced at this temperature. The I_G/I_D ratio decreases both above and below 900 °C. The carbon

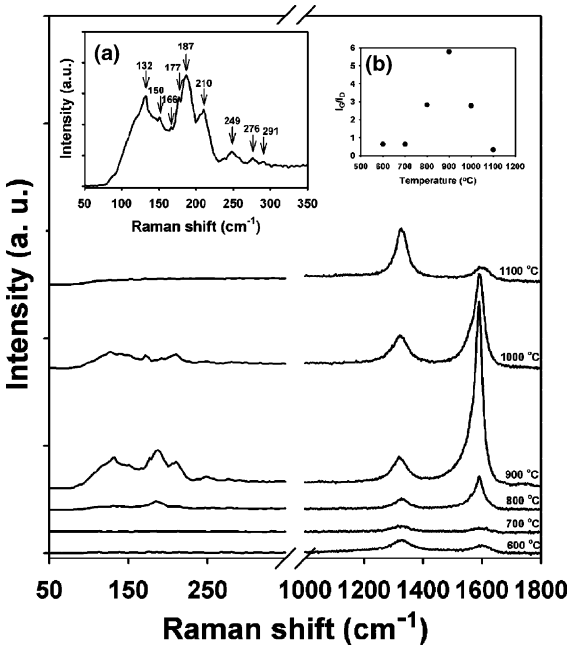

Fig. 3. Raman spectrum of CNTs deposited at different temperatures. Inset (a) enlarged view of breathing mode spectra of CNTs grown at 900 °C. Inset (b) peak intensity ratio of G band over D band as a function of temperature.

deposits at 1100 °C are the most defective, confirmed separately by a low Raman I_G/I_D ratio and by the curly nature of the carbon deposits observed in both FESEM and HRTEM.

Time dependences of the CNT growth also were studied for both 700 and 900 °C, since 700 °C appears to be the optimum growth temperature for MWCNTs and 900 °C the optimum for DWCNTs and SWCNTs. Fig. 4 shows the CNT length vs. growth duration at 700 °C. The growth appears fast at the initial stage but levels off for long durations, showing a behavior of MWCNT growth that has been observed in many CVD processes. Both the growth rate and the maximum length, however, are dependent on growth conditions [16,17,26]. Fig. 5 shows the growth-duration dependence of Raman spectroscopy performed on the surface of the CNT deposits grown at 900 °C. The major breathing mode peak positions do not change with growth duration, reflecting that the diameter distribution of CNTs does not change with increasing growth. However, the intensity ratio between the G band and the D band

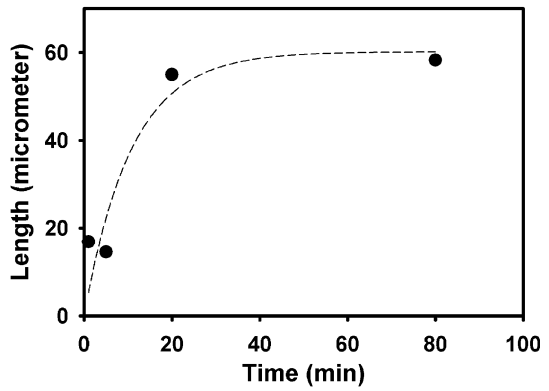

Fig. 4. CNT length as a function of growth duration at 700 °C. (The dashed line is only a guide for the eye.)

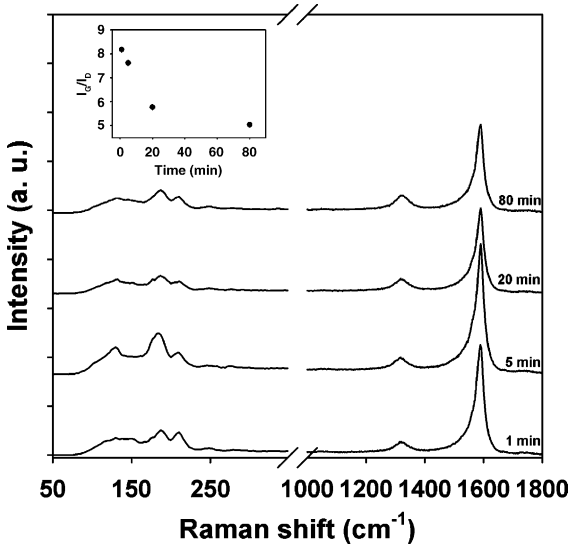

Fig. 5. Raman spectrum of CNTs for different durations of growth at 900 °C. The inset shows the peak intensity ratio of G band over D band as a function of growth duration.

dramatically *decreases* with time, as shown in the inset, suggesting that for long growth times defective carbon deposits accumulate faster than ordered graphitic structures. This result was confirmed by FESEM cross-section observations on the sample deposited for 80 min, in which amorphous carbon structures were found to have nucleated on the substrate surface.

These extensive observations using FESEM, HRTEM, and Raman spectroscopy clearly estab-

lish that the nucleation density of different forms of CNTs strongly depends on growth temperature. For MWCNTs, the nucleation density is high at low temperatures. Confinement due to neighboring CNTs forces the CNTs to grow upward and their vertical alignment is due only to this 'crowding' effect. Similar alignment has been reported using only iron film as the catalyst, without aluminum and molybdenum layers [26,27]. When the growth temperature increases, the catalyst surface roughens, as is confirmed by AFM measurements. The RMS value of the surface roughness for the catalyst surface treated at 700 °C was found to be 2 nm, lower than the RMS value of 2.5 nm at 900 °C. Aluminum was found in other work to increase the production of SWCNTs [7]. Molybdenum also has been found to effectively disperse and stabilize iron nanoparticles, and to play a role *synergetic* to the catalyst iron [3–6, 8,10,23]. Thus the substrate surface is effectively roughened and activated, and consequently nucleates large numbers of SWCNTs/DWCNTs. In fact, the nucleation density is high enough to produce small bundles of SWCNTs/DWCNTs. On the other hand, prolonged annealing treatment at 900 °C is found to encourage aggregation and the formation of large catalyst particles, and consequently to reduce the nucleation density of SWCNTs/DWCNTs. The growth-duration-dependence study of CNT growth at 900 °C described above supports this conclusion, since the large catalyst particles were found to nucleate amorphous carbon structures. The fast thermal decomposition rate accounts for the formation of defective fiber-like carbon structures at 1100 °C.

The growth-temperature range for SWCNTs and DWCNTs in this study was found to lie between 800 and 1000 °C, with an optimum at 900 °C. For SWCNTs, this temperature range is higher than was found in some other studies, in which SWCNTs have been observed at growth temperatures as low as 680 °C [8,9]. We attribute this difference to the different substrate/support materials used. In those studies, alumina and/or silica supports were employed, which had larger and still rougher surfaces than the roughened but initially flat silicon surface used here. As the study reported here illustrates, surface roughness can play an important role in stabilizing catalyst particles with smaller size and lowering the activation energy for the nucleation of SWCNTs, thus reducing the growth temperature. But the limited usefulness of this approach also is apparent, since a broad distribution of catalyst particle (and CNT) sizes always will result, and truly control of CNT type is lacking. SWCNTs have also been synthesized at high temperatures up to 1200 °C. This is partially due to the choice of carbon feedstock and has direct impact on the SWCNT quality. Amorphous carbon is generally found covering SWCNTs when C_2H_2 is used as carbon feedstock at elevated temperatures due to its fast decomposition [12,14]. In contrast, CO decomposes at a moderate rate in the high-temperature range and thus produces clean SWCNTs [10,13,19,20]. High temperature also is needed in the pyrolysis of *n*-hexane or thiophene [15,18].

In conclusion, the temperature and time dependences and the structural type of CNTs grown by CVD of C_2H_2 from a thin film of Al/Fe/Mo have been studied. The study shows that only MWCNTs nucleate at low temperatures (~700 °C) and that SWCNTs/DWCNTs nucleate starting near 800 °C. The SWCNTs/DWCNTs are optimally grown at 900 °C, where their density is sufficient to permit the aggregation of CNT bundles. Raman spectroscopy and high resolution electron microscopy indicate that growth at higher temperatures favors the formation of more defective carbon-fiber structures which are most likely caused by the higher rate of catalyst particle aggregation. The same mechanism appears responsible for the introduction of defective carbon structures at lower temperatures and much longer growth durations, indicating that optimal SWCNT/DWCNT fractional yields for this catalyst system are sensitive to both growth temperature and time.

Acknowledgements

We thank P.H. Fleming for assistance with sample preparation. This research was supported by the Laboratory Directed Research and Development Program of Oak Ridge National Laboratory (ORNL), by the Office of Basic Energy

Sciences, Division of Materials Sciences, US Department of Energy (DOE), and by the Defense Advanced Research Projects Agency under contract No. 1868HH26X1 with ORNL. The research was carried out at ORNL, managed by UT-Battelle, LLC, for the US DOE under contract No. DE-AC05-00OR22725. This research also was supported in part by an appointment (H. Cui) to the ORNL Postdoctoral Research Associates Program which is sponsored by ORNL and administered jointly by ORNL and by the Oak Ridge Institute for Science and Education under contract numbers DE-AC05-84OR21400 and DE-AC05-76OR00033, respectively.

References

[1] A. Thess, R. Lee, P. Nikolaev, H.J. Dai, P. Petit, J. Robert, C.H. Xu, Y.H. Lee, S.G. Kim, A.G. Rinzler, D.T. Colbert, G.E. Scuseria, D. Tomanek, J.E. Fischer, R.E. Smalley, Science 273 (1996) 483.
[2] A. Peigney, C. Laurent, F. Dobigeon, A. Rousset, J. Mater. Res. 12 (1997) 613.
[3] A.M. Cassell, J.A. Raymakers, J. Kong, H.J. Dai, J. Phys. Chem. B 103 (1999) 6484.
[4] M. Su, B. Zheng, J. Liu, Chem. Phys. Lett. 322 (2000) 321.
[5] Y. Li, J. Liu, Y.Q. Wang, Z.L. Wang, Chem. Mater. 13 (2001) 1008.
[6] S. Tang, Z. Zhong, Z. Xiong, L. Sun, L. Liu, J. Lin, Z.X. Shen, K.L. Tan, Chem. Phys. Lett. 350 (2001) 19.
[7] L. Delzeit, B. Chen, A. Cassell, R. Stevens, C. Nguyen, M. Meyyappan, Chem. Phys. Lett. 348 (2001) 368;
L. Delzeit, C.V. Nguyen, B. Chen, R. Stevens, A. Cassell, J. Han, M. Meyyappan, J. Phys. Chem. B 106 (2002) 5629.
[8] A.R. Harutyunyan, B.K. Pradhan, U.J. Kim, G. Chen, P.C. Eklund, Nanoletters 2 (2002) 525.
[9] G.L. Hornyak, L. Grigorian, A.C. Dillon, P.A. Parilla, K.M. Jones, M.J. Heben, J. Phys. Chem. B 106 (2002) 2821.
[10] J.H. Hafner, M.J. Bronikowski, B.R. Azamian, P. Nikolaev, A.G. Rinzler, D.T. Colbert, K.A. Smith, R.E. Smalley, Chem. Phys. Lett. 296 (1998) 195.
[11] M.D. Diener, N. Nichelson, J.M. Alford, J. Phys. Chem. B 104 (2000) 9615.
[12] B.C. Satishkumar, A. Govindaraj, R. Sen, C.N.R. Rao, Chem. Phys. Lett. 293 (1998) 47.
[13] K. Bladh, L.K.L. Falk, F. Rohmund, Appl. Phys. A: Mater. Sci. Process. 70 (2000) 317.
[14] L. Ci, S. Xie, D. Tang, X. Yan, Y. Li, Z. Liu, X. Zou, W. Zhou, G. Wang, Chem. Phys. Lett. 349 (2001) 191.
[15] H.M. Cheng, F. Li, X. Sun, S.D.M. Brown, M.A. Pimenta, A. Marucci, G. Dresselhaus, M.S. Dresselhaus, Chem. Phys. Lett. 289 (1998) 602.
[16] A.Y. Cao, X.F. Zhang, C.L. Xu, J. Liang, D.H. Wu, X.H. Chen, B.Q. Wei, P.M. Ajayan, Appl. Phys. Lett. 79 (2001) 1252.
[17] R. Andrews, D. Jacques, A.M. Rao, F. Derbyshire, D. Qian, X. Fan, E.C. Dickey, J. Chen, Chem. Phys. Lett. 303 (1999) 467.
[18] H.W. Zhu, C.L. Xu, D.H. Wu, B.Q. Wei, R. Vajtai, P.M. Ajayan, Science 296 (2002) 884.
[19] H.J. Dai, A.G. Rinzler, P. Nikolaev, A. Thess, D.T. Colbert, R.E. Smalley, Chem. Phys. Lett. 260 (1996) 471.
[20] P. Nikolaev, M.J. Bronikowski, R.K. Bradley, F. Rohmund, D.T. Colbert, K.A. Smith, R.E. Smalley, Chem. Phys. Lett. 313 (1999) 91.
[21] B. Kitiyanan, W.E. Alvarez, J.H. Harwell, D.E. Resasco, Chem. Phys. Lett. 317 (2000) 497.
[22] J. Kong, H.T. Soh, A.M. Cassell, C.F. Quate, H.J. Dai, Nature 395 (1998) 878.
[23] W.E. Alvarez, F. Pompeo, J.E. Herrera, L. Balzano, D.E. Resasco, Chem. Mater. 14 (2002) 1853.
[24] A. Jorio, R. Saito, J.H. Hafner, C.M. Lieber, M. Hunter, T. McClure, G. Dresselhaus, M.S. Dresselhaus, Phys. Rev. Lett. 86 (2001) 1118.
[25] S. Bandow, M. Takizawa, K. Hirahara, M. Yudasaka, S. Iijima, Chem. Phys. Lett. 337 (2001) 48.
[26] S.S. Fan, M.G. Chapline, N.R. Franklin, T.W. Tombler, A.M. Cassell, H.J. Dai, Science 283 (1999) 512.
[27] H. Cui, O. Zhou, B.R. Stoner, J. Appl. Phys. 88 (2000) 6072.